Continuous CO_2 capture and reduction in one process: CO_2 methanation over unpromoted and promoted Ni/ZrO_2

Lingjun Hu and Atsushi Urakawa*

Institute of Chemical Research of Catalonia (ICIQ), The Barcelona Institute of Science and Technology, Av. Països Catalans 16, 43007 Tarragona, Spain

*Email: aurakawa@iciq.es

Abstract

The recently demonstrated concept to combine CO_2 capture and utilization in one process using isothermal unsteady-state operation, namely CO_2 capture and reduction (CCR), was applied for the first time to CO_2 methanation using unpromoted and K- or La-promoted Ni/ZrO_2 catalysts. Both K and La promoters significantly improve CO_2 capture capacity and also CO_2 conversion selectivity to methane. The K-promoted catalyst ($Ni\text{-}K/ZrO_2$) captures a larger amount of CO_2 at high temperature but the capture capacity drops at low temperature due to incomplete catalyst regeneration during the cyclic unsteady-state reaction condition. In contrast, the La-promoted catalyst ($Ni\text{-}La/ZrO_2$) shows temperature-independent CO_2 capture capacity and rapid reduction of captured CO_2, thus leading to stable CCR performance. The nature of the active sites and mechanistic details were gained by TPR, reductive CO_2-TPD and space- and time-resolved *operando* DRIFTS, holistically elucidating the effects of the promoters and their impacts on CCR activity.

Keywords: CO_2 methanation, CO_2 capture and reduction, nickel catalyst, potassium, lanthanum

Introduction

Fossil fuel, the main energy source of industry and modern human life, is a two-edged sword, bringing unparalleled convenience as well as enormous CO_2 emission. The latter is considered as the culprit for global warming and climate change. Current global strategies to tackle this problem are aligned along two directions: (i) carbon capture and storage (CCS), i.e. capture CO_2 and store it in the deep underground and (ii) carbon capture and utilization (CCU), i.e. capture CO_2 and utilize it, with particularly promising paths by converting it to other useful chemicals such as methanol and methane aiming to close the carbon cycle [1-5]. Despite the increasing global efforts, risks and difficulties are perceived with the two approaches. Recent studies show that while CCS can store theoretically a vast amount of CO_2, there is a risk of releasing CO_2 back to the atmosphere [6]. Furthermore, for both CCS and CCU the common denominator is CO_2 capture process for CO_2 separation and purification, upgrading from 3-13 vol% CO_2 to relatively pure CO_2. This step is known to be costly and energy intensive [7] and most developed CO_2 conversion technologies assume this as the necessary step.

Reflecting this background, we recently developed a process combining CO_2 capture and catalytic reduction steps, so-called CO_2 capture and reduction (CCR) process. CCR is operated under isothermal, unsteady-state condition to induce the bifunctionality of catalyst. During the capture phase, CO_2 is chemically stored over catalyst, and before/upon reaching the maximum CO_2 capture capacity of the catalyst, the gas atmosphere is switched to reduction phase, such as hydrogen atmosphere to convert the stored CO_2 into a targeted product. In our first studies, a catalyst containing Cu as the main active reduction sites and K as CO_2 capture sites was developed and CCR was demonstrated with >99% CO_2 capture efficiency with diluted CO_2 effluent streams even in the presence of oxygen and water and with high conversion efficiency to CO (in practice to syngas due to the presence of unconverted hydrogen) via reverse water-gas shift reaction (RWGS) [8, 9].

Among CO_2 hydrogenation reactions, CO_2 methanation has attracted considerable interests as a path for CO_2 utilization as well as renewable energy storage [10-12]. The major advantage of producing methane is the well-established transport infrastructure through pipelines. This renders the molecule uniquely attractive for rapid and large-scale implementation of synthetic natural gas production from CO_2, as often discussed in the context of the power-to-gas scenario [13]. Recently, Farrauto *et al.* reported a Ru-based catalyst for combined CO_2 capture and methanation, showing a promising scope of unsteady-state operation [14].

In this work our efforts were directed to investigate the potential of the isothermal CCR approach for methanation reaction, particularly to understand critical material factors for efficient CO_2 capture and methane formation. Among active metal components for CO_2 methanation, nickel was chosen for its widely recognized methanation activity and its high natural abundance, whereas ZrO_2 was chosen as the support material for its good synergetic function in the reaction when used in conjunction with Ni [15, 16]. Besides K which was found effective in promoting CO_2 capture in our previous study [8, 9], the use of La was investigated for its distinct property to capture CO_2 under CCR conditions. Furthermore, the effects of each material components on the formation of active surface

species and the reaction mechanism were studied in depth by *operando* space- and time-resolved diffuse reflectance infrared Fourier transform spectroscopy (DRIFTS).

Experimental

Materials and catalyst preparation

Nickel nitrate hexahydrate (>98%, Alfa Aesar), potassium carbonate (>99%, Acros), lanthanum nitrate hexahydrate (>99.9%, Alfa Aesar), zirconium oxide (Alfa Aesar, 90 m^2 g^{-1}) were used as received. All catalyst materials were synthesized by the incipient wetness impregnation method. Ni/ZrO_2 (15/85 wt%, NZ) and Ni-La/ZrO_2 (15/5/80 wt%, NLZ) were prepared by (co)impregnating the aqueous solution of the corresponding nitrate salts onto ZrO_2. For Ni-K/ZrO_2 (15/5/80 wt%, NKZ), firstly nickel nitrate was impregnated on ZrO_2, dried overnight at 80 °C and then calcined at 500 °C for 5 h. Subsequently, the aqueous solution of K_2CO_3 was impregnated on Ni/ZrO_2. After the impregnation step, all samples were dried overnight at 80 °C and then calcined at 500 °C for 5 h.

Catalyst characterization

Powder X-ray diffraction (PXRD) was performed on D8 Advanced Powder Diffractometer (Bruker) equipped with a vertical 2theta-theta goniometer in transmission configuration, with a $K\alpha_1$ germanium monochromator for Cu radiation (λ=1.5406 Å), at a scan step of 0.02° s^{-1} from 10° to 80°.

H_2 temperature programmed reduction (H_2-TPR) was performed on TPDRO 1100 (Thermo Fisher Scientific) equipped with a TCD detector. 50 mg of catalyst material was placed in a quartz tube, pretreated at 300 °C for 30 min under N_2 flow (30 mL min^{-1}) and cooled to 30 °C under N_2. Then the gas atmosphere was changed to 5 vol% H_2 in N_2 at 30 mL min^{-1}. The sample temperature was raised from 30 to 800 °C at the ramp rate of 10 °C min^{-1} and H_2 consumption was monitored by TCD detector. Soda lime ($CaO+Na_2O$) trap was used to adsorb mainly H_2O and CO_2.

Reductive CO_2 temperature programmed desorption in H_2 atmosphere (termed as "CO_2-TPD with H_2") was conducted on TPDRO 1100. 20 mg of catalyst material was placed in a quartz tube, reduced in H_2 (5 vol% in N_2 at 20 mL min^{-1}) at 450 °C for 2 h, and then kept in He for 30 min at 50 °C. The pretreated material was further treated with CO_2 (4 vol% in He) for 1 h at 50 °C and later in He for 30 min at 50 °C. Subsequently, reductive CO_2-TPD with H_2 was performed in H_2 (5 vol% in N_2 at 20 mL min^{-1}) under ramping from 50 to 700 °C at the rate of 10 °C min^{-1}. The composition of the effluent gas and concentration (only qualitatively) during the ramp were monitored by online mass spectrometer (Omnistar, Pfeiffer Vacuum).

Catalytic reaction

Catalysts were first pelletized, crushed and sieved into the size of 200-300 μm. 1 g of catalyst material was charged into a tubular reactor made of stainless steel, fixed with quartz wool and pre-reduced in pure H_2 (50 mL min^{-1}) at 450 °C for 1 h. Then the reactor was cooled down to a desired reaction temperature (250, 300, 350 or 450 °C) in He and the catalyst was evaluated for CCR. During the CO_2 capture phase 4.7 vol% CO_2 (>99.9998%, Abelló Linde) in He and during the reduction phase pure H_2 (>99.999%, Abelló Linde), both at 50 mL min^{-1} for ca. 5 min for each phase, were alternately passed

through the reactor at the ambient pressure. The flow sequence was controlled by a computer-controlled switching valve which was synchronized with the gas detection. Time-resolved quantitative gas analysis of CO_2, CO and CH_4 was performed by transmission IR spectroscopy using a gas cell mounted in ALPHA FT-IR spectrometer (Bruker), giving a time-resolution of ca. 2.5 s. To improve the signal to noise ratio (S/N) of the gas species detection, six CCR cycles were evaluated for each catalyst and each experimental condition and the concentration profiles were averaged into one CCR cycle after ensuring that the concentration profiles at every cycle are reproducible.

Space- and time-resolved DRIFTS

Space- and time-resolved *operando* DRIFTS was performed using a reaction cell mimicking the action of a fixed-bed plug flow reactor, with a similar design to that reported previously [17]. The cell was mounted in a Praying Mantis optical accessory (Harrick) fixed in Vertex 70V FTIR spectrometer (Bruker). 200 mg catalyst sieved in 75–150 µm particle size was charged into the channel on the cell (2 x 2 mm^2 cross section) to form a catalyst bed with ca. 10 mm length and also fixed by quartz wool. Prior to DRIFTS measurement, catalyst was pre-reduced in pure H_2 with at 10 ml min^{-1} at 350 °C for 2 h. The catalyst was treated under a CCR condition at 350 °C with repeated CCR cycles (5 vol% CO_2 in He vs. pure H_2 at 10 mL min^{-1}) for ca. 12-15 h to activate and stabilize the catalyst for CCR. Then the catalyst was cooled down to a desired temperature (250, 300 or 350 °C) to perform DRIFTS under a CCR condition (each phase of ca. 200 s). 55 spectra were collected per phase at 4 cm^{-1} resolution with a liquid N_2 cooled MCT detector at four positions along the axial direction of the catalyst bed (we call these positions: Front, Middle 1, Middle 2 and Back). DRIFTS measurement was performed for 9 CCR cycles at each position of the catalyst bed and the last 7 or 8 cycles were averaged into one cycle for the detailed analysis. The composition of the effluent stream was analyzed by mass spectrometer (OmniStar, Pfeiffer Vacuum) and in the gas cell of the ALPHA IR spectrometer (Bruker) in a synchronized manner with the DRIFTS measurements.

Results and discussion

For the sake of more straightforward discussions on the catalyst structure-activity relationships, first catalytic performance is described, followed by *ex situ* and *in situ*/*operando* characterization of the catalysts and reactive surface species.

CCR performance of unpromoted and K- or La-promoted Ni/ZrO_2 catalysts

In this study, sufficiently long CO_2 capture and reduction periods were used to compare the performance of the catalyst materials investigated. In practice, by shortening the periods, one can optimize a CCR process by maximally avoiding release of uncaptured CO_2 and waste of H_2, respectively [8]. It is worth noting that matching the duration of CO_2 capture and reduction periods is important for process intensification using a two-reactor system [8]. The aim of this work is to understand the roles of promoters in CCR and thus no process optimization was attempted.

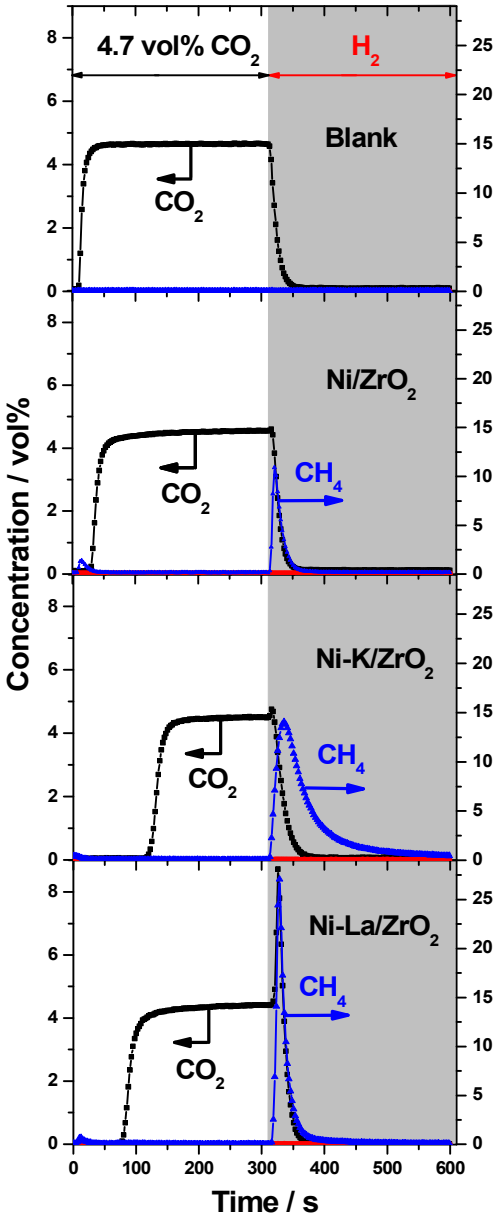

Figure 1. Effluent concentration profiles of CO_2 (black) and reduction products, CH_4 (blue) and CO (red) during CO_2 capture (white area, 4.7vol% CO_2 in He, 50 mL min^{-1}) and reduction (grey area, pure H_2, 50 mL min^{-1}) phases over Ni/ZrO_2 (NZ), $Ni\text{-}K/ZrO_2$ (NKZ) and $Ni\text{-}La/ZrO_2$ (NLZ) at 350 °C and atmospheric pressure. Blank test was performed at room temperature without charging catalyst in the reactor to show the concentration profile without any reaction.

Figure 1 shows representative CO_2, CH_4 and CO concentration profiles during CCR with Ni/ZrO_2 (NZ), $Ni\text{-}K/ZrO_2$ (NKZ) and $Ni\text{-}La/ZrO_2$ (NLZ) at 350 °C. As reference, the concentration profiles using the empty reactor at room temperature (Figure 1, top panel, Blank) are also shown. At 350 °C, mainly CH_4 was formed as the product and little CO was detected for all catalysts examined. The CH_4 selectivity (the rest is CO selectivity)

was 89, 98 and 99% for NZ, NKZ and NLZ, respectively. For comparison, we performed CO_2 hydrogenation under steady-state conditions (4 vol% CO_2 and 50% H_2 in He at 100 mL min^{-1} at atmospheric pressure) using the same catalysts (Supporting Information, Table S1). The major difference between the catalytic performance under steady- and unsteady- state operation is the function of K where selectivity to CO was notably increased under steady-state conditions (43 and 24% CO selectivity at 250 and 350 °C, respectively), while this was not the case under unsteady-state conditions where high selectivity (>90%) to CH_4 was achieved for NKZ. The steady-state selectivity characteristics are in agreement with the previous findings where potassium enhances CO selectivity of Ni catalysts by lowering the activation energy for CO formation [18, 19]. This indicates that the catalytic properties can be largely altered and the distinct reactivity can arise by the unsteady-state operation.

Most strikingly, prominent effects of the K and La promoters on the dynamic CO_2 capture and reduction processes were evidenced. When K was used as promoter, the CO_2 capture efficiency (i.e. how much CO_2 was captured on the catalyst during the whole capture phase) was drastically increased from 11% (NZ) to 44% (NKZ) as evident from the full CO_2 capture for ca. 30 s for NZ and for ca. 120 s for NKZ. On the other hand, the La promoter was not as effective as K, and the CO_2 capture efficiency of NLZ was 32% (ca. 80 s full capture). In all cases, the increase in CO_2 concentration after saturation is rapid and steep. This concentration profile indicates highly active and efficient CO_2 capture of these materials and this is one of the most important characteristics to be a CCR catalyst.

Very large differences were observed for CH_4 formation during the reduction phase. Due to the differences in the amount of captured CO_2, consequently the amount of CH_4 produced during the reduction phase was increased by 4-fold and 2-fold for NKZ and NLZ, respectively, in comparison to NZ. Also, the duration to decrease and reach 1 vol% CH_4 concentration in the reduction phase was comparable for NZ (ca. 40 s) and NLZ (ca. 60 s), whereas that for NKZ was significantly longer (170 s) as evident from the tailing concentration profile observed for NKZ (Figure 1). As mentioned earlier, the duration of the reduction period with respect to that of the CO_2 capture period is of paramount importance for process intensification. When two CCR reactors are used for continuous CO_2 capture by switching the functions of the two reactors (capture or reduction), the durations for CO_2 capture and reduction should be matching. In case of NKZ, the reduction time is remarkably longer by ca. 50 s than full CO_2 capture duration under the condition evaluated. This means that the capture phase should be switched to the reduction phase much before full utilization of CO_2 capture capacity. In this regard, NLZ performs more suitably for CCR process under the duration of ca. 60 s capture/reduction period where the catalyst's capture capacity is more efficiently exploited, while the duration is sufficient for catalyst regeneration for the subsequent CO_2 capture. This shorter reduction period also implies more efficient use of H_2 by minimizing the release of unreacted H_2 in the effluent. Nevertheless, it should be noted that the CO_2 capture capacity and reduction duration vary significantly by the reaction conditions such as temperature and space velocity and they should be optimized for the most promising catalyst for practical applications.

Another important observation was the release of unreacted CO_2 during the reduction phase (Figure 1). The larger amount of CO_2 release for NLZ is evident from Figure 1. The

amounts of unreacted, released CO_2 in the reduction phase with respect to those captured in the capture phase were 14% (NZ), 7% (NKZ) and 21% (NLZ). This means that for NLZ about 80% of captured CO_2 was converted to CH_4 and the rest was released as CO_2. The coverage of hydrogen atoms over Ni is known to restrain CO_2 adsorption [20] and the differences in the amount of released CO_2 in the reduction phase may stem from distinct interactions between hydrogen and CO_2 with Ni for the three catalysts. However, *operando* DRIFTS studies presented later indicate that the differences of CO_2 release among the three catalysts likely reflect the material-dependent mechanism of CO_2 capture and active surface species present over the catalyst surfaces.

Furthermore, CCR performance of the three catalysts was evaluated in the range of 250-450 °C and the results are summarized in Figure 2 (the CCR profiles are presented in Supporting Information, Figure S1). As mentioned earlier, the catalytic performance are highly experimental-condition-dependent; therefore they are for indicative and comparative purposes only. NZ displayed the poorest catalytic performance among the three with the lowest CO_2 conversion. Significant decrease in CH_4 selectivity from 96 to 73% was observed as the temperature was increased from 250 to 450 °C, while the CO_2 conversion remained almost constant at 20%. Upon K-promotion (NKZ), both CO_2 conversion as well as CH_4 selectivity have improved drastically. Remarkably, the selectivity to CH_4 was >95% in the evaluated temperature range, while CO_2 conversion was highly temperature-dependent because the function of K for CO_2 capture is greatly enhanced at higher temperatures, up to ca. 60% at 450 °C (Supporting Information, Figure S1). NLZ, on the other hand, presented also high CH_4 selectivity (>90%), notably with almost constant CO_2 conversion (ca. 35%) in the temperature range. The latter seems decreased slightly at higher temperatures (Figure 2) and this is attributed to the enhanced release of unreacted CO_2 during the reduction phase at higher temperatures (Supporting Information, Figure S1). Depending on the determining factor of a process (e.g. CO_2 capture capacity, faster reduction duration and operation temperature), one can choose more suitable catalyst composition; NKZ for high temperature operation while NLZ for low or varying temperature operation.

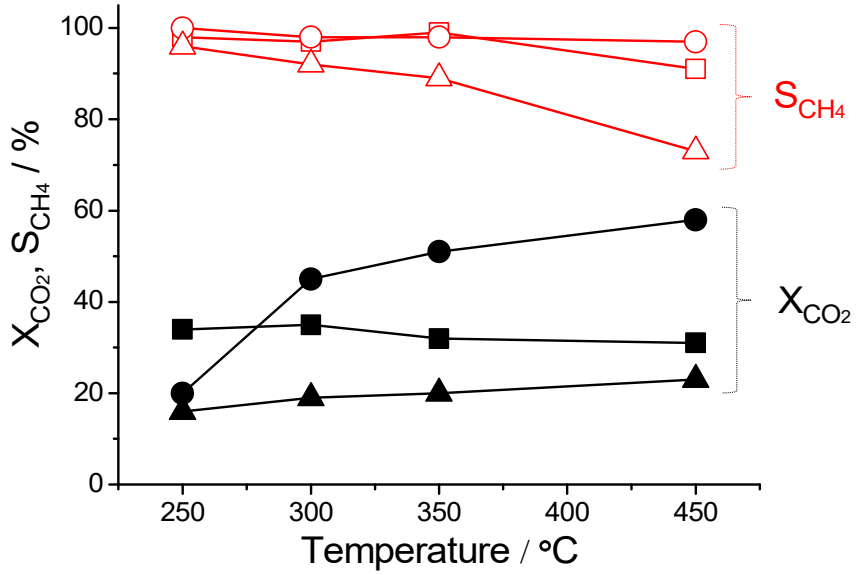

Figure 2. CO_2 conversion (X_{CO2}) and CH_4 selectivity (S_{CH4}) for Ni/ZrO_2 (triangle), $Ni-K/ZrO_2$ (circle) and $Ni-La/ZrO_2$ (square) at different temperatures under the CCR operation (1 g catalyst, 4.7% CO_2 in He vs. H_2 at 50 mL min^{-1}).

Catalyst characterization

The structure of the three catalysts before (labelled as fresh) and after the CCR (labelled as spent) was studied by X-ray diffraction (Figure 3). Most reflections present in the XRD patterns belong to monoclinic ZrO_2 (JCPDS: 00-036-0420). The only difference engendered by the reaction is that nickel oxide (JCPDS: 00-047-1049) in the fresh catalysts is reduced to the metallic form (JCPDS: 01-087-0712). This is reasonable since the reaction was terminated after the reduction phase. La and K, which are expected to exist as La_2O_3 and K_2CO_3, respectively, based on synthesis condition were not detectable by XRD. Considering the rather high loading of the two components (5 wt%), the results indicate high dispersion of these species as nanocrystallites or in amorphous phase, which may be responsible for the prominent promoter effects observed in CCR.

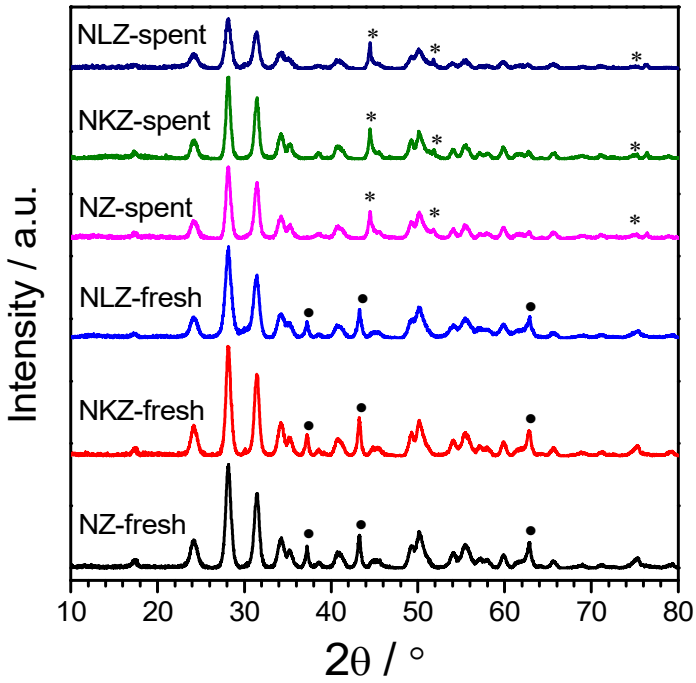

Figure 3. XRD patterns of Ni/ZrO_2 (NZ), Ni-K/ZrO_2 (NKZ) and Ni-La/ZrO_2 (NLZ) before ("fresh") and after ("spent") the CCR. (•) nickel (II) oxide and (*) metallic nickel.

Figure 4 shows H_2-TPR results of the three catalysts. For all materials, an agglomerated broad reduction peak starting at ca. 300 °C was observed. The reducibility of Ni is similar for NZ and NKZ, with some differences in the presence of high temperature peaks for NKZ. The reduction profile of NLZ is markedly different from those of the other two catalysts, exhibiting a sharp peak at ca. 350 °C. According to literature, the reduction peak at low temperature is related to relatively free (i.e. unbound) NiO which shows higher reducibility while the one at high temperature is attributed to reduction of complex NiO_x species due to the metal-support interactions [21, 22]. Based on this interpretation, we can conclude that the metal-support interactions between Ni and ZrO_2 are similar for NZ and NKZ, whereas they can be largely altered by the La-promotion, leading to enhanced reducibility of NiO. The excellent catalytic activity of NLZ at low temperature may be due to the high reducibility of Ni, thus attaining high conversion efficiency of captured CO_2 and high selectivity to CH_4.

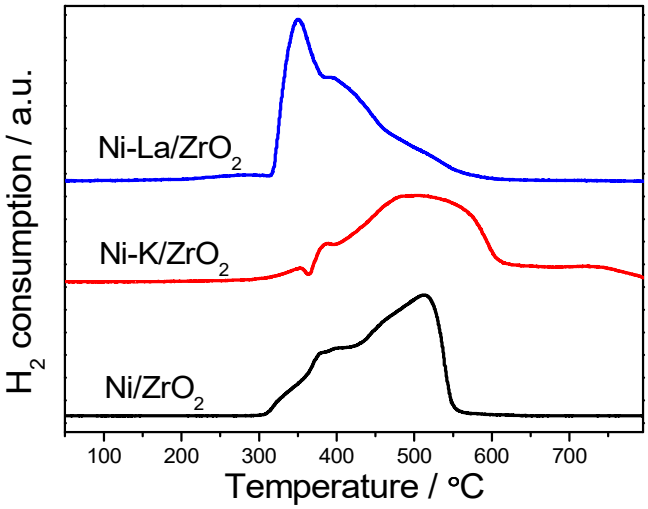

Figure 4. H_2-TPR profiles of Ni/ZrO_2, $Ni\text{-}K/ZrO_2$ and $Ni\text{-}La/ZrO_2$.

To understand better the temperature-dependent catalytic activity and CCR properties of the catalysts, reactive (reductive) CO_2-TPD in the presence of 5 vol% H_2 was performed with simultaneous analysis of released gaseous products by mass spectrometry (MS). Figure 5 (top panel) shows the TCD signal of the temperature-programmed experiments. All catalysts presented three main peaks with largely different characteristics due to surface species desorption and/or gaseous product formation, and the MS profiles (Figure 5, lower three panels) clarifies the origin of the peaks.

Interestingly, the first peak observed for all catalysts is due to an uptake of H_2 taking place at ca. 100-150 °C without H_2O formation (not shown). In case of NLZ and NKZ, these peaks are overlapped with another broad one due to CO_2 desorption as confirmed by the MS profiles. This CO_2 desorption was not observed for NZ and this originates from the presence of the K/La promoter.

At slightly above 200 °C, NZ and more prominently NLZ showed another peak due to CH_4 formation. In contrast, for NKZ the formation of CH_4 was observed starting at 300 °C in a wider temperature range, indicating the higher stability of the surface species formed by CO_2 capture on NKZ. The sharpness of the CH_4 peak of NLZ compared to NKZ is in accordance with the faster reduction profile observed in CCR (Figure 1). It is worth pointing out that the CH_4 peak was observed at lower temperature for NLZ compared to NZ, which is in accordance with the H_2-TPR results, showing the higher reducibility of NLZ than NZ. Besides, there is another peak due to CH_4 formation at even higher temperature (>500 °C) for all catalysts. The amount of CH_4 formed at this high temperature was minor compared to the former one. Surprisingly, there was a formation of CO observed only for NKZ. Only a small amount of CH_4 was formed for NZ and NLZ, but a large amount of CO was formed for NKZ starting its formation at 550 °C and ending at 800 °C. This is likely due to the formation of a highly stable potassium carbonate species, which was reduced to CO by H_2. This indicates that some portion of K components may be present as stable carbonates and do not participate in the reaction during CCR and that NKZ likely exhibits much lower

CH_4 selectivity at >500 °C due to more favorable CO formation. The results are in full accordance with the large temperature-dependence of the CCR performance of NKZ and the less temperature-dependence of NLZ and its high CCR activity at low temperature.

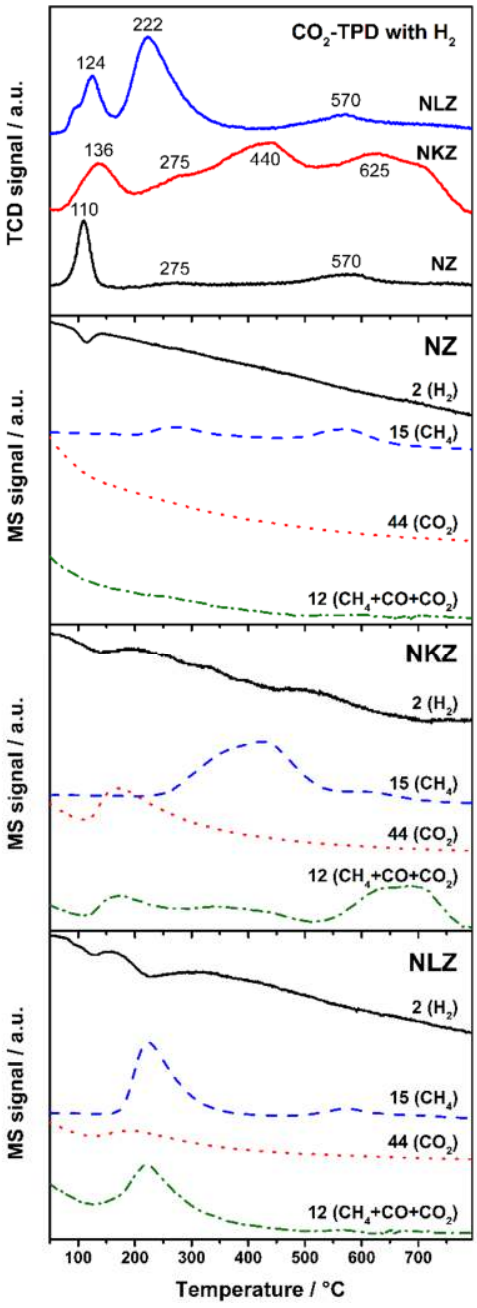

Figure 5. (top panel) Reactive (reductive) CO_2-TPD profiles with H_2 of Ni/ZrO_2, $Ni\text{-}K/ZrO_2$ and $Ni\text{-}La/ZrO_2$. (lower three panels) The MS signals observed during the CO_2-TPD with H_2. The number and formula in brackets represent the mass to charge ratio (m/z) and the corresponding plausible chemicals.

Space- and time-resolved operando DRIFTS

With the convincing observations and evidences of the promoter effects, we further investigated the effects of the promoters on the formation and evolution of surface species along the axial direction of the catalyst bed by DRIFTS. Time-resolved DRIFTS spectra were measured at equally-spaced 4 positions along the catalyst bed. It should be noted that the last spectrum of the reduction phase, where the catalyst surface is likely the cleanest during the CCR cycle, was taken as the internal background to calculate the DRIFT spectra. In other words, if there are surface species stably present during CCR, e.g. stable potassium carbonate as indicated before, the spectral feature will not appear and only those responding to the CCR unsteady-state condition and responsible for CCR chemistry appear in the spectra.

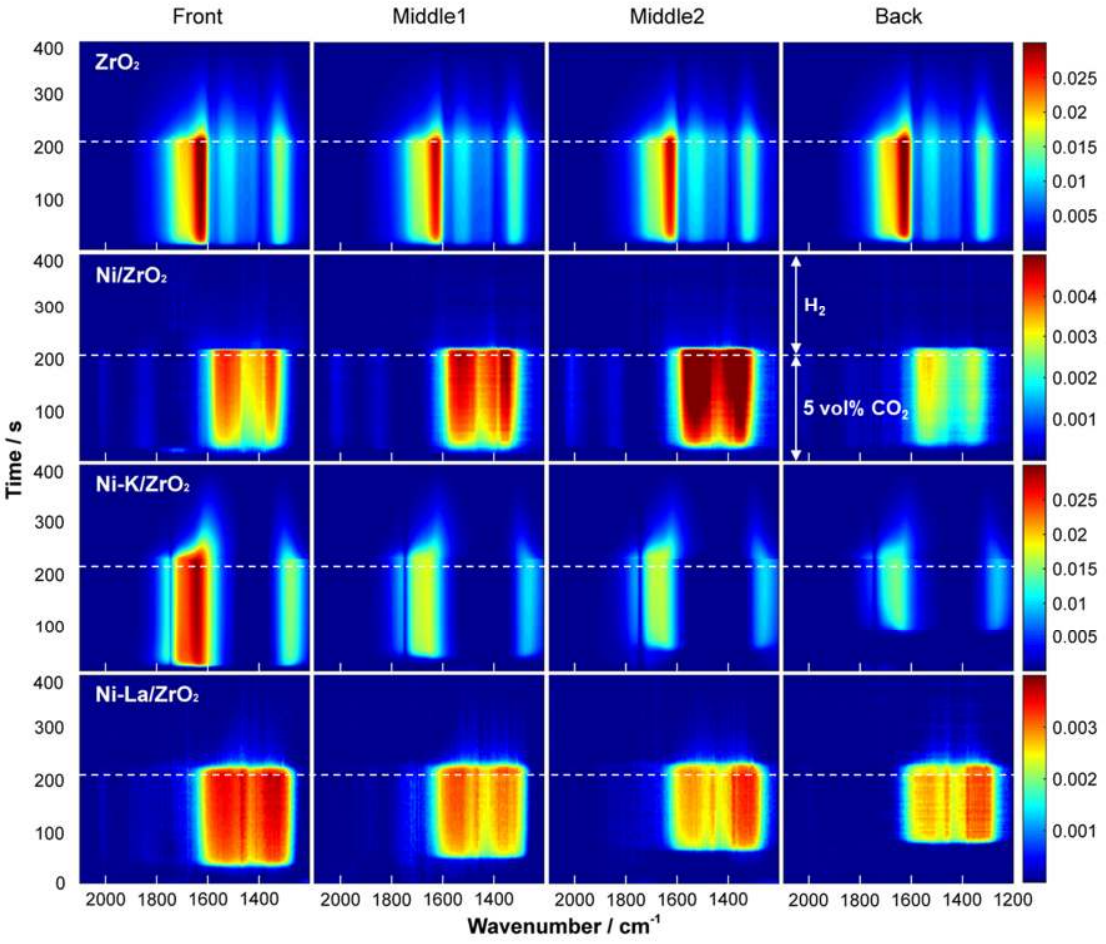

Figure 6. Space- and time-resolved *operando* DRIFT spectra of ZrO_2, Ni/ZrO_2, $Ni\text{-}K/ZrO_2$ and $Ni\text{-}La/ZrO_2$ at 350 °C under the CCR condition (5 vol% CO_2 in He vs. pure H_2, both at 10 mL min^{-1}). The last spectrum of the CCR cycle was taken as the background. The scale is shown in absorbance unit.

Figure 6 shows the evolution of surface species during CCR for the three catalysts and also for ZrO_2 which was also evaluated as a comparative reference. For the ZrO_2 support,

the main bands observed during the capture phase were at 1320, 1420, 1522 and 1629 cm^{-1}, which can be assigned to bicarbonate and carbonate species formed over ZrO_2 [23]. After impregnating Ni on the support (i.e. NZ), the spectral features changed completely; these bands disappeared and the bands of formate species (1351 and 1521 cm^{-1}) and weakly bound carbonate species (1400 cm^{-1}) appeared in the capture phase [23, 24]. The La-promoted catalyst (NLZ) exhibited similar spectral features to those of NZ with some band broadening likely caused by the strong interaction between Ni and La which impacts on the reducibility of Ni (Figure 4). It is interesting to note that some signatures of adsorbed CO species on Ni (linear one at 2013 cm^{-1} and bridged one at 1850 cm^{-1}) were observed for NZ and NLZ [25, 26]. This indicates that the Ni surface is reduced and exposed during the CCR. In contrast, K-promotion (NKZ) totally changed the type of surface species formed during the capture phase with the formation of the bands possibly assigned to formyl species (1760 cm^{-1}) and bidentate carbonate (1277 and 1657 cm^{-1}) [27, 28]. The former is generally considered as a plausible intermediate for CO_2 methanation [27]. The above insights provide a strong evidence that the function of K and La promoters in capturing CO_2 on the catalyst surface are chemically completely different. Although the ZrO_2 support can chemically trap CO_2, methane production was negligible below 300 °C. At 350 °C, the methane yield rose to 3%, but this is notably lower compared to the methane yields over NZ (19%), NKZ (51%) and NLZ (36%) under the same reaction condition, showing the clear importance of Ni for efficient conversion to methane and also of the K/La promoters for CO_2 capture.

There are two important observations one can make based on the space-resolved approach. The first one is the travelling of the so-called CO_2-capture front, i.e. a gradual movement of position towards the back position where CO_2 capture (surface species formation) starts, which is more clearly visible for NKZ and NLZ (CO_2 concentration profiles extracted from DRIFTS data are shown in Supporting Information, Figure S2). On the other hand, such CO_2 capture front is not clearly visible for ZrO_2 and NZ, indicating less aggressive CO_2 capture over these materials. The second important observation is the spatial gradient of the amount of surface species formed upon CO_2 capture as indicated by the value of absorbance (i.e. color in Figure 6) along the catalyst bed. For ZrO_2, the amount of surface species is homogeneously distributed over the catalyst bed, while a very large concentration gradient of surface species was observed for NZ and NKZ and to a lesser extent for NLZ. It is important to notice that most of the CO_2 capture processes take place near the front position of the catalyst for NKZ, whereas NLZ captures CO_2 throughout the catalyst bed with much less concentration gradient of the surface species.

In the reduction phase, the formed surface species are consumed completely, forming CH_4 and releasing CO_2, whose amounts vary depending on the catalyst. The action of reductive transformation of surface species is very distinct for the two contrasting catalysts, NKZ and NLZ. In case of NKZ, the reductive transformation starts at all positions but very slowly by gradually consuming surface species for CH_4 formation. On the other hand, the reduction process of NLZ is a fast process with a drastic decrease in the concentration of the surface species, forming a slight but firm reduction front (reducing the surface species step-by-step towards the back position). Such a reduction profile is ideal for CCR process since most of the H_2 is consumed for the transformation and thus H_2 utilization efficiency is high.

Conclusions

CO_2 methanation by Ni-based catalysts using the isothermal unsteady-state operation, enabling CO_2 capture and conversion steps in one process, i.e. CO_2 capture and reduction (CCR) approach, was investigated. The roles of two promoters, K and La, to Ni/ZrO_2 in CO_2 capture as well as CO_2 conversion to methane were studied and their functions were elucidated by H_2-TPR, reductive CO_2-TPD in H_2 atmosphere and space- and time-resolved *operando* DRIFTS. First, all Ni-based catalysts are highly selective in CH_4 formation. The K-promotion is more effective in enhancing CO_2 capture capacity, but the capacity and consequently the CCR performance deteriorates at low temperature. In contrast, the La-promotion affords to enhance CO_2 capture capacity moderately and importantly to convert the captured CO_2 very rapidly to CH_4 with high H_2 utilization efficiency as evidenced by space- and time-resolved DRIFTS. The TPR and TPD studies show that the La-promoter improves reducibility of Ni without changing the reaction mechanism from that of Ni/ZrO_2, forming active formate intermediate species for CH_4 production. On the other hand, the K-promotion altered the reaction mechanism completely where formyl species cooperated with bidentate carbonates are the active surface species which are more difficult to be reduced by H_2 to CH_4. This study firmly shows the possibility to achieve high CO_2 conversion and high CH_4 selectivity at low temperature (e.g. 250 °C) using $Ni\text{-}La/ZrO_2$ and in contrast at increased capacity using $Ni\text{-}K/ZrO_2$ at high temperature (efficiently at >350 °C) by the CCR approach. The K-promoted catalyst binds CO_2 strongly and is advantageous in avoiding the release of unreacted CO_2 during the reduction phase. This work shows clearly the distinct advantages of the two promoters to the Ni catalyst in CCR operation and is expected to open further discussions and technical evaluation of CCR process in comparison to the conventional, two-step CO_2 capture and conversion approach.

Acknowledgements

We thank the Generalitat de Catalunya for financial support through the CERCA Programme and recognition (2014 SGR 893) and MINECO (CTQ2016-75499-R (AEI/FEDER-UE)) for financial support and support through Severo Ochoa Excellence Accreditation 2014–2018 (SEV-2013-0319). Repsol and Dr. Jordi Ampurdanés are acknowledged for lending us some of the equipments used and experimental support for space- and time-resolved DRIFTS, respectively.

References

[1] J. Gibbins, H. Chalmers, Energy Policy 36 (2008) 4317-4322.
[2] J.T. Litynski, S.M. Klara, H.G. McIlvried, R.D. Srivastava, Environ. Int. 32 (2006) 128-144.
[3] C. Song, Catal. Today 115 (2006) 2-32.
[4] P.J. Lunde, F.L. Kester, Ind. Eng. Chem. Proc. DD 13 (1974) 27-33.
[5] A. Álvarez, A. Bansode, A. Urakawa, A.V. Bavykina, T.A. Wezendonk, M. Makkee, J. Gascon, F. Kapteijn, Chem. Rev. 117 (2017) 9804-9838.
[6] M. Lenzen, Crit. Rev. Environ. Sci. Technol. 41 (2011) 2169-2185.
[7] R. Snieder, T. Young, GSA Today 19 (2009) 36-37.

[8] L.F. Bobadilla, J.M. Riesco-García, G. Penelás-Pérez, A. Urakawa, J. CO2 Util. 14 (2016) 106-111.
[9] T. Hyakutake, W. van Beek, A. Urakawa, J. Mater. Chem. A 4 (2016) 6878-6885.
[10] W. Wei, G. Jinlong, Front. Chem. Sci. Eng. 5 (2011) 2-10.
[11] C. Mebrahtu, S. Abate, S. Perathoner, S. Chen, G. Centi, Catal. Today 304 (2018) 181-189.
[12] F. Wang, S. He, H. Chen, B. Wang, L. Zheng, M. Wei, D.G. Evans, X. Duan, J. Am. Chem. Soc. 138 (2016) 6298-6305.
[13] J. Guilera, J.R. Morante, T. Andreu, Energ. Convers. Manage. 162 (2018) 218-224.
[14] S. Wang, E.T. Schrunk, H. Mahajan, R.J. Farrauto, Catalysts 7 (2017).
[15] K. Zhao, W. Wang, Z. Li, J. CO2 Util. 16 (2016) 236-244.
[16] D.C.D. da Silva, S. Letichevsky, L.E.P. Borges, L.G. Appel, Int. J. Hydrogen Energ. 37 (2012) 8923-8928.
[17] A. Urakawa, N. Maeda, A. Baiker, Angew. Chem. Int. Ed. 47 (2008) 9256-9259.
[18] M.T. Duignan, E. Grunwald, S. Speiser, J. Phys. Chem. 87 (1983) 4387-4394.
[19] T.K. Campbell, J.L. Falconer, Appl. Catal. 50 (1989) 189-197.
[20] J. Wambach, G. Illing, H.J. Freund, Chem. Phys. Lett. 184 (1991) 239-244.
[21] H.-S. Roh, K.-W. Jun, W.-S. Dong, J.-S. Chang, S.-E. Park, Y.-I. Joe, J. Mol. Cat. A 181 (2002) 137-142.
[22] S. Li, C. Zhang, Z. Huang, G. Wu, J. Gong, Chem. Commun. 49 (2013) 4226-4228.
[23] H. Takano, Y. Kirihata, K. Izumiya, N. Kumagai, H. Habazaki, K. Hashimoto, Appl. Surf. Sci. 388 (2016) 653-663.
[24] N.M. Gupta, V.S. Kamble, V.B. Kartha, R.M. Iyer, K.R. Thampi, M. Gratzel, J. Catal. 146 (1994) 173-184.
[25] H. Muroyama, Y. Tsuda, T. Asakoshi, H. Masitah, T. Okanishi, T. Matsui, K. Eguchi, J. Catal. 343 (2016) 178-184.
[26] S.-i. Fujita, M. Nakamura, T. Doi, N. Takezawa, Appl. Catal. A 104 (1993) 87-100.
[27] C. Schild, A. Wokaun, A. Baiker, J. Mol. Cat. 69 (1991) 347-357.
[28] F. Solymosi, H. Knozinger, J. Catal. 122 (1990) 166-177.

Supporting Information

Continuous CO_2 capture and reduction in one process: CO_2 methanation over unpromoted and promoted Ni/ZrO_2

Lingjun Hu and Atsushi Urakawa*

Institute of Chemical Research of Catalonia (ICIQ), The Barcelona Institute of Science and Technology, Av. Països Catalans 16, 43007 Tarragona, Spain

*Email: aurakawa@iciq.es

Table S1. Catalytic performance of Ni/ZrO_2, $Ni\text{-}K/ZrO_2$ and $Ni\text{-}La/ZrO_2$ for steady-state CO_2 hydrogenation (4 vol% CO_2 and 50% H_2 in He at 100 mL/min at atmospheric pressure)

Catalyst (wt%)	CO_2 conversion/%			CH_4 selectivity/%		
	250 °C	350 °C	450 °C	250 °C	350 °C	450 °C
NZ(15/85)	13	86	99	100	99	99
NKZ(15/5/80)	12	50	86	57	76	95
NLZ(15/5/80)	58	100	97	95	100	98

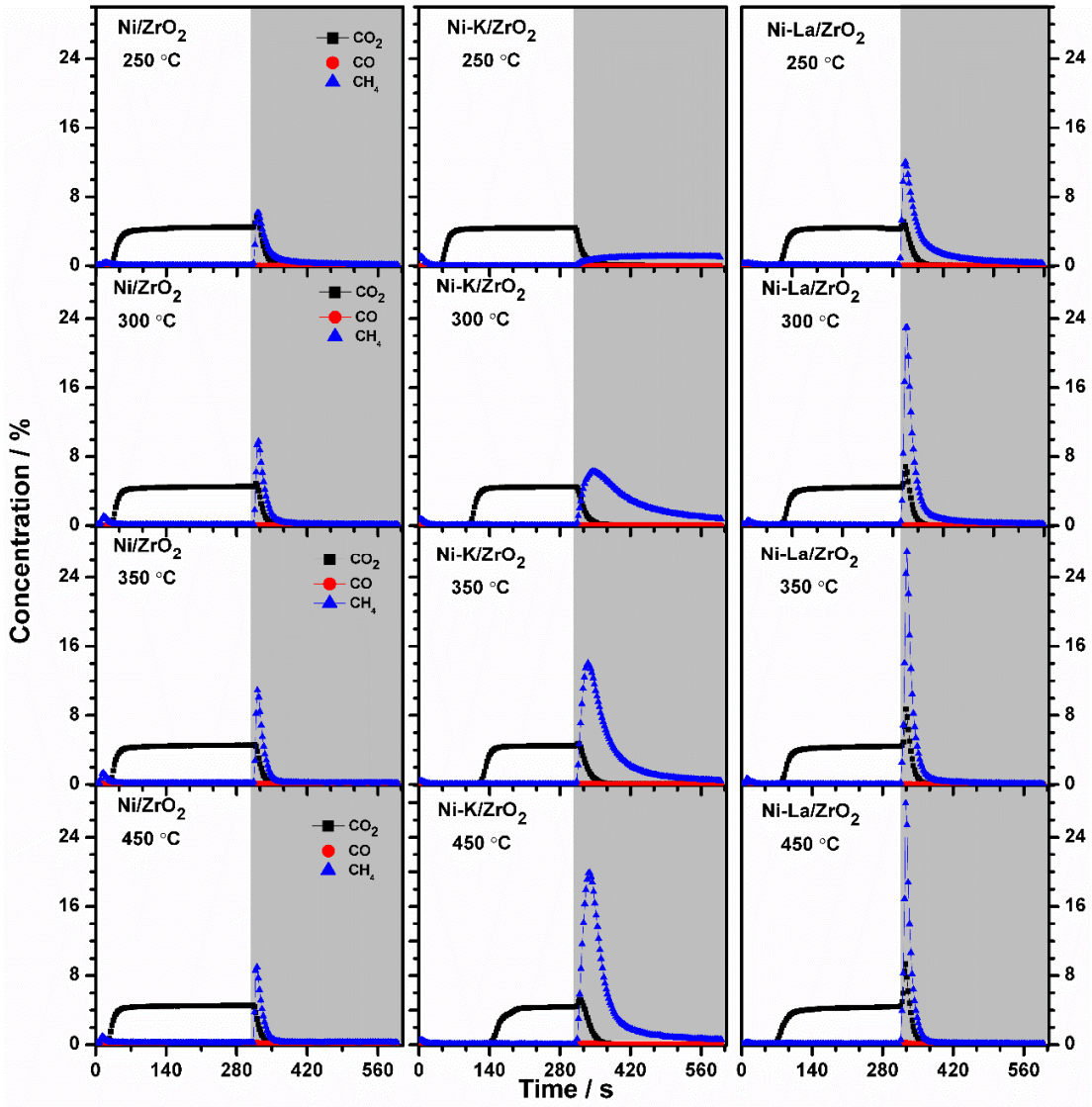

Figure S1. Concentration profiles of CO_2 and reduction products (CH_4 and CO) during CO_2 capture (white area, 4.7 vol% CO_2 in He, 50 mL min^{-1}) and reduction (grey area, pure H_2, 50 mL min^{-1}) processes over the three Ni-based catalysts at different temperatures and atmospheric pressure.

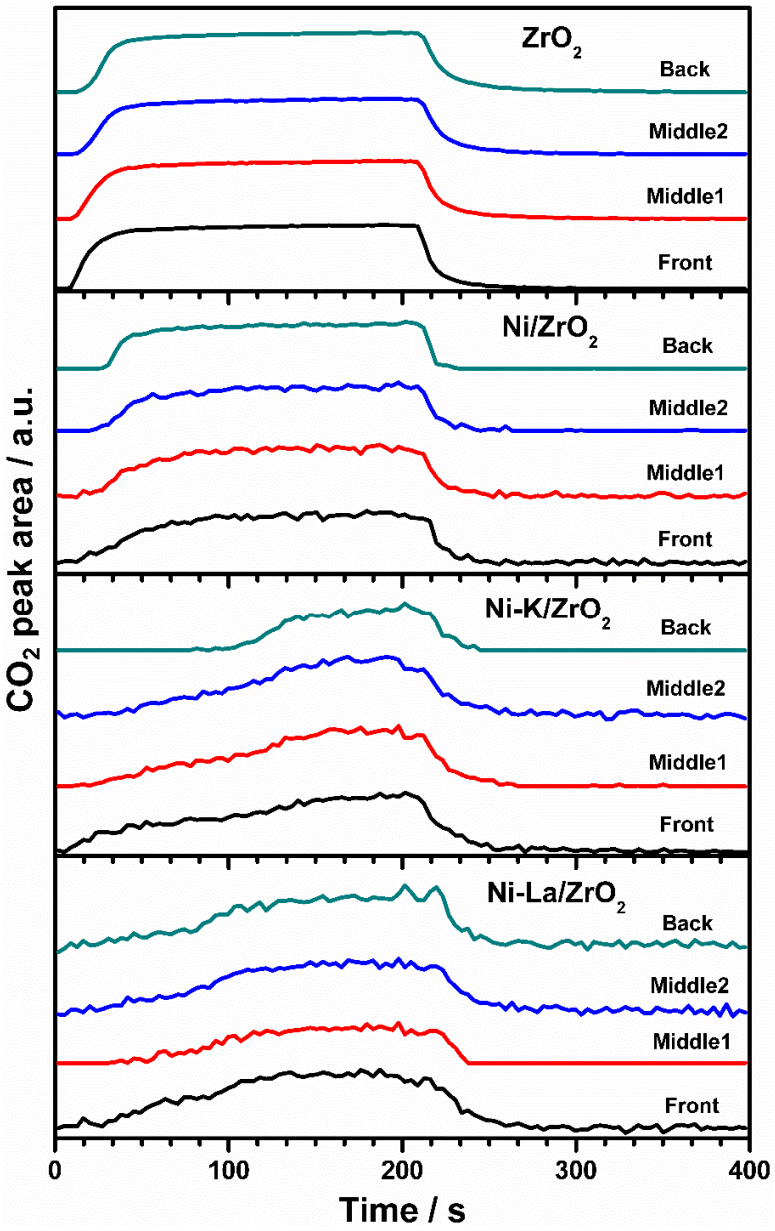

Figure S2. Temporal evolution of the band area of gas phase CO_2 extracted from space- and time-resolved DRIFT spectra acquired at 350 °C at the four positions.